

# Synthesis of Surfactant-Templated Silica Films with Orthogonally Aligned Hexagonal Mesophase

Venkat R. Koganti and Stephen E. Rankin\*

Chemical and Materials Engineering Department, University of Kentucky, Lexington, Kentucky 40506-0046

Received: October 30, 2004; In Final Form: December 10, 2004

Thin silica films with orthogonally aligned hexagonal close-packed cylindrical structure are synthesized by dip coating silica precursors and poly(ethylene oxide)–polypropylene oxide (PEO–PPO) triblock surfactants (P123) onto modified glass slides. All films cast from this sol display 2D hexagonal pore structures ( $a \sim 6.2$  nm) under transmission electron microscopy (TEM). However, X-ray diffraction (XRD) shows that confining freshly deposited films between two chemically neutral modified slides completely aligns the pores toward the direction orthogonal to the substrate. Equally effective alignment is obtained by using slides modified with either a random PEO–PPO copolymer or P123 itself. The channels in films cast onto unmodified slides, onto modified slides which are exposed to air, or onto modified slides which are exposed to unmodified glass slides align at least partially parallel to the substrate. Parallel mesophase alignment is also observed in a control experiment with a sol containing the nonionic surfactant template decaethylene glycol hexadecyl ether (Brij-56) sandwiched between copolymer-modified slides because the surfaces are not chemically neutral toward Brij-56. This study confirms that it is possible to use substrate surface chemistry to control the orientation of mesophases in mixtures of reactive silicates and low molecular weight nonionic surfactant templates.

## Introduction

Since mesoporous ceramic films with 2D hexagonal close packed (HCP) cylindrical pores were first prepared by surfactant-templated coating processes,<sup>1,2</sup> researchers have sought methods to prepare HCP cylindrical pore structures oriented orthogonal to the films.<sup>3,4</sup> This orientation would provide an array of well-defined, unidirectional, and uniformly sized pores with a minimal path length through the film. Like the close-packed pore arrays of anodized alumina, this structure could be used for many applications including membrane separations, sensor components, and nanoscale templates for arrays of nanorods, nanotubes, and other structures.<sup>5,6</sup> Electrochemical etching of the oxide layer of aluminum is an established method to produce large uniform arrays of cylindrical pores in chemically and thermally robust films.<sup>7,8</sup> However, the size of the pores in anodized alumina is limited to the range from 10 to 100 nm.<sup>9,10</sup>

Dip coating of ceramic precursors with self-organizing pore templates (such as surfactants or block copolymers) offers an alternative approach to the synthesis of thin nanoporous metal oxide films.<sup>11</sup> This is a rapid, controllable technique, and removal of the structure directing agents from these films leaves uniform, ordered pores comparable to the size of the micelle templates (in the range of 2–10 nm). Using cationic and nonionic surfactants, Lu et al.<sup>2</sup> were first able to conclusively demonstrate the formation of films with well-ordered 2D HCP arrays of cylindrical channels. However, application of these materials for nanotemplating is limited because preferential interactions between the headgroups of the surfactant molecules and the substrate aligns these cylindrical channels parallel to the substrate.<sup>2</sup> This parallel orientation makes the pores inaccessible. Cubic bicontinuous pore structures have been used as

an alternative to achieve accessible pores.<sup>12,13</sup> However, bicontinuous pore structures allow diffusion to occur laterally in addition to the preferred direction and therefore cannot be used to prepare arrays of isolated nanostructures. Orthogonally aligned cylindrical channels are needed for nanotemplating and for avoiding lateral diffusion. Forming these structures by surfactant templating provides a direct route to a wider range of pore sizes, pore spacing, and matrix materials than have been obtained using anodized alumina.

It has been shown that the macroscopic orientation of 2D HCP mesoporous silica domains within the plane of the film can be controlled by using flow fields and substrate topology.<sup>14–16</sup> Partial orthogonal alignment has been achieved by using flow fields to generate arrays of topological defects,<sup>17</sup> by seeding the films with nanoparticles,<sup>18</sup> or by using controlled evaporation.<sup>5</sup> However, none of these methods has permitted complete orthogonal alignment of the pores. Truly orthogonal pores were recently reported by growing SBA-15 (mesoporous silica prepared using PEO–PPO triblock copolymer as template) within the pores of anodized alumina.<sup>19</sup> This approach takes advantage of the parallel alignment of the surfactant micelles at the surface of the alumina pores, but presents the SBA-15 mesopores over only a fraction of the area, and still necessitates an alumina matrix. If the orientation of the micelles were controlled during synthesis, we should be able to create pure silica (or other metal oxide) films.

Examples of orthogonal thin film mesostructure alignment are available in the diblock copolymer literature. Electric fields,<sup>20–22</sup> directional crystallization,<sup>23</sup> solvent vapor treatment,<sup>24</sup> chemically patterned surfaces<sup>25–29</sup> and engineered surface topography<sup>30,31</sup> have all been successfully used to align the microdomains in block copolymer films. In addition to these methods, simulations have shown that one can align anisotropic mesophases perpendicular to the substrates by eliminating preferential interactions between the blocks of the amphiphile

\* To whom correspondence should be addressed. Phone: 1-859-257-9799. E-mail: srankin@engr.uky.edu.

and the substrate. This approach has processing advantages because it requires no specialized field-generating equipment or lithographic pattern generating methods. Both self-consistent field theory and Monte Carlo simulations have suggested that AB block copolymer lamellar mesophases should align parallel to walls that interact with a strong preference for either block.<sup>32–35</sup> Neutral walls, which have no strong preference for either block, align the lamellae perpendicular to the walls.<sup>33–35</sup> A more recent density functional theory study confirms the same trend for asymmetric block copolymers which form HCP mesophases.<sup>36</sup> Monte Carlo simulations of Rankin et al. confirm that orthogonal alignment is predicted for short nonionic surfactant HCP mesophases confined between chemically neutral walls.<sup>37</sup>

The theoretical predictions about the effects of substrate chemistry on block copolymer mesophases orientation have been beautifully confirmed by the preparation of orthogonally aligned polystyrene–poly(methyl methacrylate) (PS–PMMA) block copolymer films in a number of studies by Russel and co-workers.<sup>38–41</sup> However, all of the polymers used have high molecular weights (70 000–80 000), so even if one block is selectively removed to create pores,<sup>40</sup> the spacings are still on the order of >20 nm. To the best of our knowledge, no one has yet reported using a chemically neutral surface to align the anisotropic mesophases in surfactant-templated ceramics. Substrate surface chemistry has been explored only by comparing films prepared on the hydrophobic surface of graphite to those prepared on hydrophilic surfaces such as mica and silica. Consistent with the predictions of simulations,<sup>37</sup> the HCP channels align parallel to the substrate whether the surface is hydrophilic or hydrophobic.<sup>42</sup> Orthogonal alignment should be achieved on a chemically neutral surface, as we test here. Pai et al. recently suggested that because mesophases formation coincides with silica polycondensation, the possibility to align and manipulate mesophases may be limited for surfactant-templated sol–gel films.<sup>43</sup> However, Cagnol et al. were able to modulate the phase of cetyltrimethylammonium bromide (CTAB)-templated silica by adjusting the humidity after film deposition.<sup>44</sup> We hypothesize that the mobility of silicates after dip coating is sufficient to allow mesophase reorientation when chemically neutral surfaces are present.

We will use triblock surfactant P123 as a pore template, which has an average composition  $\text{HO}(\text{C}_2\text{H}_4\text{O})_{20}(\text{C}_3\text{H}_6\text{O})_{70}(\text{C}_2\text{H}_4\text{O})_{20}\text{H}$ . Zhao et al. have previously used P123 to prepare thin films with 2D HCP pore structure (oriented parallel to silicon wafers) by dip coating.<sup>45</sup> Our strategy will be to modify glass slides by cross-linking a thin film of PEO–PPO random copolymer on their surfaces or by cross-linking a thin film of the template copolymer itself on their surfaces. Both of these modification procedures will result in chemically neutral surfaces for the P123 templating agent which we use, but the average size of the PEO and PPO domains on the modified surfaces differs between them. We will show that, under the right conditions, these modified slides can be used to prepare orthogonally oriented P123–silica films with HCP mesophases structures.

## Experimental Section

Before coating, all of the borosilicate glass substrates were cleaned in a 7:3 mixture of concentrated  $\text{H}_2\text{SO}_4$  (96–98 wt %) and 30% aqueous  $\text{H}_2\text{O}_2$ . Some of the slides were then modified by cross-linking either P123 or a PEO–PPO random copolymer. To a solution of 0.415 mM random copolymer in acetone was added a drop of glycerol to act as a cross-linker. An equimolar amount of 1,6-diisocyanohexane (DH) was then added dropwise

to this mixture under constant stirring. The resulting solution was dip-coated onto clean glass slides, and the slides were aged at 120 °C overnight to drive the isocyanate–hydroxyl reaction to completion. The same procedure was used to cross-link P123 using 0.696 mM copolymer.

The coating solution was prepared by addition of a solution of P123 to a prehydrolyzed silica sol following the procedure of Liu et al.<sup>11</sup> First, tetraethoxysilane (TEOS), ethanol, water, and HCl (mole ratio 1:3.8:1:( $5 \times 10^{-5}$ )) were refluxed at 70 °C for 90 min. Then, the remaining water and HCl were added, increasing the concentration of HCl to 7.34 mM. After stirring this mixture at 25 °C for 15 min, the sols were aged at 50 °C for 15 min. The required amount of P123 was dissolved in ethanol, and this solution was added to the above aged silica sol with constant stirring. The final mole ratios were 1:22:5:0.004:0.01 TEOS: $\text{C}_2\text{H}_5\text{OH}$ : $\text{H}_2\text{O}$ :HCl:P123. Slides were dip-coated with this sol at a withdrawal speed of 7.6 cm/min. Plain or modified slides were used as substrates. After coating a modified slide, an identically modified slide was placed in contact with one side of the freshly coated slide. The films were then aged and dried at 40 °C for 24 h and at 100 °C for 24 h. To explore the effect of the relation between the surface and the surfactant chemistry, films were also prepared under identical conditions, but with Brij-56 (primarily  $\text{HO}(\text{C}_2\text{H}_4\text{O})_{10}\text{C}_{16}\text{H}_{33}$ ) replacing P123 in the sol. The mole ratio of Brij-56:TEOS was 0.0555:1. In the discussion below, P123 will be the surfactant unless Brij-56 is specifically mentioned.

The thickness of each film was measured using a Dektak 6M Stylus profilometer with a diamond stylus. X-ray diffraction (XRD) patterns were collected with a Siemens (D-5000) diffractometer using Cu K $\alpha$  radiation ( $\lambda = 1.54098 \text{ \AA}$ ). The thin films were analyzed in Bragg–Brentano geometry without further preparation. Pieces of mesoporous film were scraped off the slides and deposited onto lacey carbon transmission electron microscopy (TEM) grids. TEM images were recorded on either a JEOL 2000FX or a JEOL 2010F microscope operated at 200 kV.

P123 (BASF), Brij-56 (Aldrich), TEOS (>99%, Fluka), deionized ultrafiltered water (Fisher), anhydrous ethanol (Aaper Alcohol & Chemical), acetone (HPLC grade, Fisher), glycerol (99+%, Aldrich), DH (98+%), and random copolymer (75% EO,  $M_n \sim 12\,000$ , Aldrich) were all used as received.

## Results and Discussion

We start by confirming that the sol forms 2D hexagonal close packed cylindrical channels in films cast onto unmodified slides under the conditions used. Following the procedure described above, we were able to prepare transparent films without any macroscopic defects after deposition and drying by using P123 as a structure-directing agent. The thickness of the films was found to be 240 nm using the profilometer. Figure 1a shows the XRD pattern of material which was coated on an unmodified glass slide. We can clearly see the (100) reflection and its second-order reflection. The  $d$  spacing of the (100) planes is around 5.5 nm. Unlike powder products which show all HCP reflections, no (110) reflection is observed due to preferential orientation of (100) planes parallel to the substrate.<sup>46</sup> This observation is consistent with what others have reported for hexagonal phases, and we have confirmed that the pore structure is stable after calcination at 550 °C for 4 h in air (results not shown).

We modified some of the glass slides by cross-linking a thin film of PEO–PPO random copolymer on their surfaces. We then coated these modified slides with the silica sol. A similarly

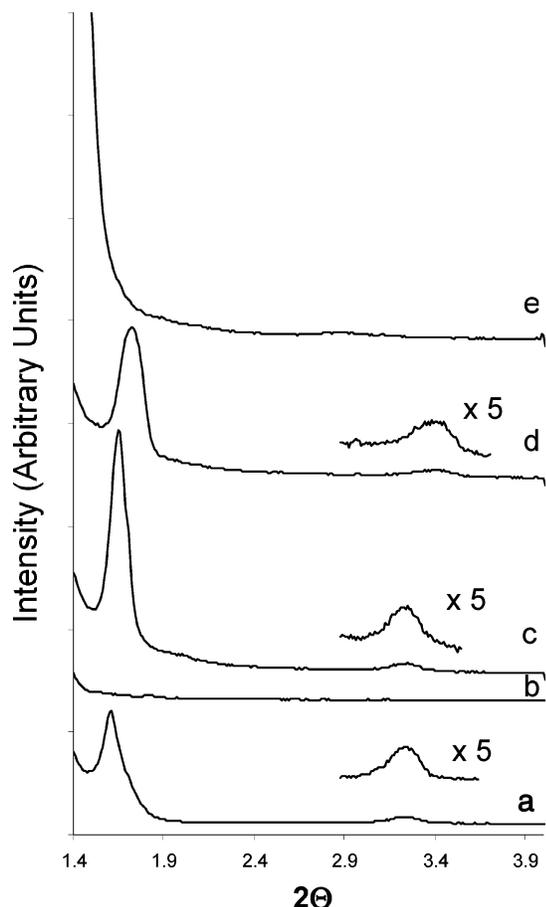


**Figure 1.** XRD patterns of P123-templated silica films coated on an unmodified slide (a); coated on a slide on which random copolymer was cross-linked before coating and exposed to (b) a similarly modified slide or (c) air; or coated on a slide on which P123 was cross-linked before coating and exposed to (d) air or (e) a similarly P123-modified slide. The patterns were offset vertically for clarity, and trace e was cut off at a value above which no features are seen.

modified slide was placed in contact with the coated slide immediately after coating and kept there during drying and aging. Parts b and c of Figure 1 show the XRD patterns obtained from two different sides of the same modified, coated slide. The side which was in contact with a similarly PEO-ran-PPO modified slide showed no reflections in the XRD pattern (Figure 1b), while the other side of the slide displays two well-resolved peaks corresponding to the (100) plane and its second-order reflection (Figure 1c). Similar to the film coated on an unmodified slide, the (100)  $d$  spacing for this material (on the side not sandwiched with another modified slide) is 5.5 nm. The thicknesses of this and the other films cast onto modified slides were in the range of  $240 \pm 5$  nm, consistent with the films prepared on unmodified slides. There was no evidence in the thickness profiles of any silica film being pulled off when the slides were separated after aging.

As described by Hillhouse et al., when the HCP cylindrical mesostructure is oriented perpendicular to the substrate, we do not expect to see any peaks in the XRD pattern because the scattering vector does not lie in the plane of the sample in conventional Bragg–Brentano geometry.<sup>46</sup> However, the HCP phase does not need to be perfectly perpendicular to the substrate; HCP domains can have a distribution of angles with respect to the substrate and still show no reflections. Thus, the absence of XRD reflections from a film that was confined between two random PEO–PPO copolymer modified surfaces during aging only demonstrates that the HCP phase is oriented

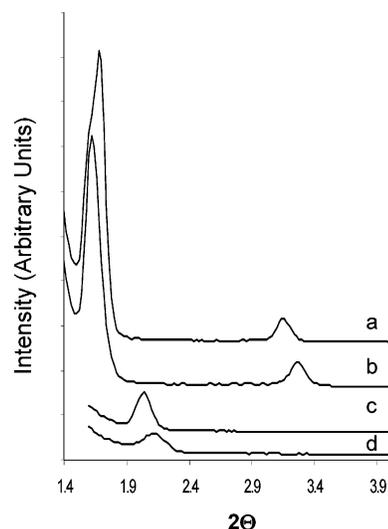


**Figure 2.** XRD patterns of P123-templated silica thin films (a) coated on a random copolymer-modified slide and exposed to an unmodified slide or (b) coated on a P123-modified slide and exposed to an unmodified slide. XRD patterns of Brij-56-templated films (c) coated on a random copolymer-modified slide and exposed to a similarly modified slide or (d) coated on a P123-modified slide and exposed to a similarly modified slide.

orthogonally away from the plane of the substrate. The presence of a significant amount of parallel-oriented domains would give rise to detectable reflections.

The second way that we modified the surface of the slides was to cross-link a thin film of the template copolymer itself (P123) on the surface before coating it with the silica sol. This was done as a test to see whether the blockiness of the PEO and PPO groups on the modified surface influences the ability of the copolymer to act as a neutral surface. The simulations that predicted perpendicular orientation were based on chemically uniform surfaces,<sup>32–37</sup> so it was unknown how the size of the surface modifier blocks would affect orientation. During aging, the film was again confined between identical modified surfaces. Figure 1e shows the XRD pattern obtained from the side which was kept in contact with a similarly modified slide. It does not have any reflections, as opposed to the side which was in contact with air (Figure 1d). For the side in contact with air, the  $d_{100}$  spacing is 5.2 nm. The absence of reflections in Figure 1e shows that a surface modified with polymer blocks whose size is comparable to that of the surfactant template can still act as a chemically neutral surface for the alignment of mesostructures.

To see if the absence of reflections in films sandwiched between modified slides was just because of confinement or if it was really a surface effect, we coated some silica films on modified slides (random copolymer or P123 modified) and placed an unmodified glass slide in contact with the films immediately after coating. The film was thus sandwiched between one chemically neutral surface and one hydrophilic surface during aging. Figure 2a shows the XRD pattern from a film sandwiched between one random PEO–PPO copolymer modified slide and one unmodified slide. Figure 2b shows the XRD pattern from a film sandwiched between one P123-modified slide and one unmodified slide. In both cases we can clearly see the (100) reflection and its second-order reflection. The  $d_{100}$  in Figure 2a is 5.2 nm and in Figure 2b is 5.5 nm. This demonstrates that it is important to sandwich these films between two chemically neutral surfaces in order to observe complete orthogonal alignment.

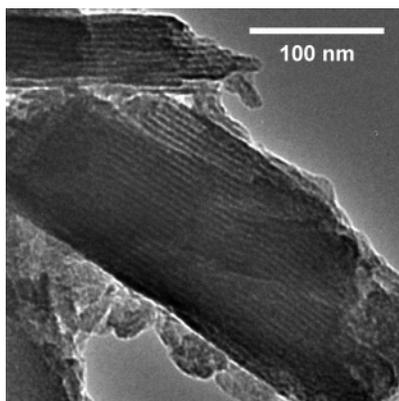


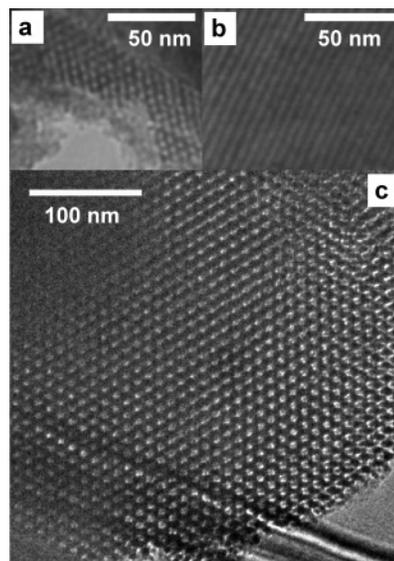
**Figure 3.** TEM image of sample coated on unmodified slide and scraped off.

To confirm that chemical neutrality of the substrate is the reason for the orthogonal alignment, we also prepared silica films in which P123 was replaced with the nonionic surfactant Brij-56. This surfactant has a short PEO headgroup and a short alkane tail, rather than a PPO tail. The small size of the surfactant compared to the PEO–PPO blocks, and its different tail chemistry, should cause different interactions with a modified surface than are seen for P123. Figure 2c shows that the Brij-56-templated film sandwiched between random copolymer-modified slides gives a distinct reflection consistent with the hexagonal phase of Brij-56-templated films with the channels aligned parallel to the substrate.<sup>2</sup> Figure 2d shows the same parallel orientation for a Brij-56-templated film sandwiched between P123-modified slides. These observations demonstrate the importance of the modified surface being designed so that it is neutral toward the specific chemistries present in the surfactant template that is being used.

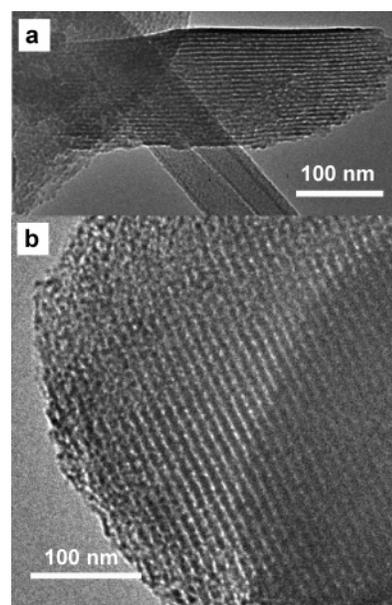
Up to this point, we have been taking the loss of X-ray reflections as an indicator of orthogonal alignment. The absence of X-ray reflections provides better statistical evidence for orthogonal alignment than TEM, since films with some orthogonal alignment sometimes also contain domains with parallel alignment.<sup>5,17</sup> However, X-ray reflections could also disappear if the long-range order were simply lost. We differentiate between these possibilities by using TEM to directly image the pore ordering in the material. An XRD pattern from a modified surface showing no peaks coupled with TEM images which show hexagonal ordering is sufficient for us to conclude that we have a 2D HCP pore structure oriented orthogonal to the substrate.

Figure 3 shows the TEM image of material removed from an unmodified slide. The piece of film shown contains close-packed cylindrical channels, which in Figure 3 are viewed from the edge. The  $d$  spacing obtained from XRD is consistent with the channel spacing in the TEM images. This confirms that we form a well-ordered 2D HCP cylindrical phase on unmodified slides using P123 as a template with the recipe described above. The (100) and (200) reflections in the XRD pattern indicate that the (100) plane of cylinders in the HCP structure lies parallel to the substrate.<sup>46</sup>

Figure 4 shows the TEM image of material obtained by scraping material from a slide which was modified with cross-linked PEO-ran-PPO. Parts a and b of Figure 4 are two views of material removed from the film which was dried and aged between two modified slides. We can clearly see regions with hexagonal cylindrical patterns (Figure 4a) and stripe patterns showing that we have channels rather than spherical pores (Figure 4b). These images show that the absence of XRD



**Figure 4.** TEM images of pieces of P123-templated silica thin film scraped from the random copolymer-modified glass substrate. Panels a and b are two views of the material scraped from the film sandwiched between two random copolymer-modified slides, and c is a view of the material scraped from the side exposed to air.



**Figure 5.** TEM images of pieces of P123-templated silica thin film scraped from the cross-linked P123-modified glass substrate: (a) material scraped from the film sandwiched between two cross-linked P123-modified slides, and (b) material scraped from the side exposed to air.

reflections is not due to loss of order, but to alignment of the cylindrical pores orthogonal to the substrate. The TEM image of material removed from the other side of the same film (which was in contact with air) shows the same well-defined HCP structure (Figure 4c).

We have also modified the surface of glass slides by cross-linking P123 itself on the surface. A representative TEM image of the material scraped off from the side of a slide which was confined with another P123-modified slide is shown in Figure 5a. This image, along with the absence of reflections in the XRD pattern obtained from this same side of the film, confirms that we are able to prepare a 2D HCP mesophase orthogonal to the surface. Figure 5b shows that the same HCP pore structure

is also found on the side of the film aged in air, even though the XRD pattern indicates parallel pore alignment for this side of the film.

Taken together, the above results show that when the surface of a glass slide is modified by cross-linking PEO-PPO copolymers with blocks shorter than or the same size as the template copolymer (random copolymer- and P123-modified surfaces, respectively), one can align the 2D hexagonal close packed cylindrical mesophases in the direction orthogonal to the substrate. However, to see complete orthogonal alignment, it appears to be important to sandwich the freshly deposited film with another modified slide. Films cast on modified slides but exposed to either air (a hydrophobic surface) or unmodified glass (a hydrophilic surface) show at least partial mesophase alignment parallel to the substrate. It is likely that these films actually have an orthogonally aligned layer near the modified substrate. However, preference for one block at the air-film or glass-film interface probably creates a parallel layer near that surface. Also, the experiment with Brij-56 shows how important it is to have modified surfaces that are chemically neutral toward the specific template being used to prepare the film. Either because of the small size of the PEO and alkane segments in Brij-56 or because the modified surfaces have a net attraction for PEO blocks of Brij-56, we observe parallel mesophase alignment of Brij-56-templated films sandwiched between modified slides.

## Conclusions

In this brief paper we have demonstrated the preparation of oriented 2D hexagonal close packed cylindrical channels in 240 nm thick P123-templated silica films. We have successfully implemented the idea from molecular simulations that confinement of a nonionic surfactant mesophase between chemically neutral surfaces will align the cylindrical pore channels in the direction orthogonal to the substrate. A combination of XRD and TEM characterization confirmed the preservation of the HCP structure and its orientation out of the plane of the substrate. Both random PEO-PPO and the surfactant itself (P123) have been cross-linked to create chemically neutral surfaces. At this stage, we found it essential to sandwich the films between two chemically modified surfaces to induce complete orthogonal alignment. Contact of one surface of the film with either air or unmodified glass caused a loss of orthogonal alignment. Since the films were all originally cast with one side exposed to air, this suggests that the as-deposited films are able to reorient while aging in contact with a pair of chemically modified surfaces. These films are promising structures for a variety of applications, and in the future we plan to present more detailed studies of the compositional variety allowed by these films and further characterization of their properties.

**Acknowledgment.** The authors thank Bing Tan for gathering the data with the JEOL 2010F microscope. The authors gratefully acknowledge financial support from the U.S. Department of Energy Grant No. DE-FG02-03ER46033 and from NSF Grant No. DMR-0210517.

## References and Notes

- Ogawa, M. *Supramol. Sci.* **1998**, *5*, 247–251.
- Lu, Y.; Ganguli, R.; Drewien, C. A.; Anderson, M. T.; Brinker, C. J.; Gong, W.; Guo, Y.; Soyez, H.; Dunn, B.; Huang, M. H.; Zink, J. I. *Nature* **1997**, *389*, 364–368.
- Pevzner, S.; Regev, O.; Rozen, R. Y. *Curr. Opin. Colloid Interface Sci.* **2000**, *4*, 420–427.
- Eidler, K. J.; Roser, S. J. *Int. Rev. Phys. Chem.* **2001**, *20*, 387–466.
- Ryan, K. M.; Erts, D.; Olin, H.; Morris, M. A.; Holmes, J. D. *J. Am. Chem. Soc.* **2003**, *125*, 6248–6288.
- Chik, H.; Xu, J. M. *Mater. Sci. Eng., R* **2004**, *43*, 103–138.
- Konno, M.; Shindo, M.; Sugawara, S.; Saito, S. *J. Membr. Sci.* **1987**, *37*, 193–197.
- Masuda, H.; Fukuda, K. *Science* **1995**, *268*, 1466–1468.
- Diggle, J. W.; Downie, T. C.; Goulding, C. W. *Chem. Rev.* **1969**, *69*, 365.
- Xu, T.; Zangari, G.; Metzger, R. M. *Nano Lett.* **2002**, *2*, 37–41.
- Brinker, C. J.; Lu, Y. F.; Sellinger, A.; Fan, H. Y. *Adv. Mater.* **1999**, *11*, 579.
- Xomeritakis, G.; Braunbarth, C. M.; Smarsly, B.; Liu, N.; Kohn, R.; Klipowicz, Z.; Brinker, C. J. *Microporous Mesoporous Mater.* **2003**, *66*, 91–101.
- Nishiyama, N.; Park, D. H.; Koide, A.; Egashira, Y.; Ueyama, K. *J. Membr. Sci.* **2001**, *182*, 235–244.
- Hillhouse, H. W.; Okubo, T.; van Egmond, J. W.; Tsapatsis, M. *Chem. Mater.* **1997**, *9*, 1505–1507.
- Hillhouse, H. W.; van Egmond, J. W.; Tsapatsis, M. *Langmuir* **1999**, *15*, 4544–4550.
- Miyata, H.; Kuroda, K. *Chem. Mater.* **2000**, *12*, 49–54.
- Hillhouse, H. W.; van Egmond, J. W.; Tsapatsis, M.; Hanson, J. C.; Larese, J. Z. *Chem. Mater.* **2000**, *12*, 2888–2893.
- Klotz, M.; Albouy, P.-A.; Ayrat, A.; Menager, C.; Grosso, D.; Van der Lee, A.; Cabuil, V.; Babonneau, F.; Guizard, C. *Chem. Mater.* **2000**, *12*, 1721–1728.
- Lu, Q.; Gao, F.; Komarneni, S.; Mallouk, T. E. *J. Am. Chem. Soc.* **2004**, *126*, 8650–8651.
- Thurn-Albrecht, T.; DeRouchey, J.; Russell, T. P.; Jaeger, H. M. *Macromolecules* **2000**, *33*, 3250–3253.
- Elhadj, S.; Woody, J. W.; Niu, V. S.; Saraf, R. F. *Appl. Phys. Lett.* **2003**, *82*, 871–873.
- Morkved, T. L.; Lu, M.; Urbas, A. M.; Ehrichs, E. E.; Jaeger, H. M.; Mansky, P.; Russell, T. P. *Science* **1996**, *273*, 931–933.
- Park, C.; De Rosa, C.; Lotz, B.; Fetters, L. J.; Thomas, E. L. *Macromol. Chem. Phys.* **2003**, *204*, 1514–1523.
- Fukunaga, K.; Elbs, H.; Magerle, R.; Krausch, G. *Macromolecules* **2000**, *33*, 947–953.
- Rockford, L.; Liu, Y.; Mansky, P.; Russel, T. P.; Yoon, M. *Phys. Rev. Lett.* **1999**, *82*, 2602–2605.
- Rockford, L.; Mochrie, S. G.; Russel, T. P. *Macromolecules* **2000**, *34*, 1487–1488.
- Kim, S. O.; Solak, H. H.; Stoykovich, H.; Ferie, N. J.; de Pablo, J. J.; Nealey, P. F. *Nature* **2003**, *424*, 411–414.
- Li, Z.; Qu, S.; Rafailovich, M. H.; Sokolov, J.; Tolan, M.; Turner, M. S.; Wang, J.; Schwarz, S. A.; Lorenz, H.; Kotthaus, J. P. *Macromolecules* **1997**, *30*, 8410–8419.
- Turner, M. S.; Joanny, J. F. *Macromolecules* **1992**, *25*, 6681–6689.
- Fasolka, M. J.; Harris, D. H.; Mayes, A. M.; Yoon, M.; Mochrie, S. J. *Phys. Rev. Lett.* **1997**, *79*, 3018–3021.
- Sivaniah, E.; Hayashi, Y.; Iino, M.; Hahimoto, T.; Fukunaga, K. *Macromolecules* **2003**, *36*, 5894–5896.
- Kikuchi, M.; Binder, K. *J. Chem. Phys.* **1994**, *101*, 3367–3377.
- Brown, G.; Chakrabarti, A. *J. Chem. Phys.* **1994**, *102*, 1440–1448.
- Pickett, G. T.; Balazs, A. C. *Macromolecules* **1997**, *30*, 3097–3103.
- Matsen, M. W. *J. Chem. Phys.* **1997**, *106*, 7781–7791.
- Huinink, H. P.; Brokken-Zijp, J. C. M.; van Dijk, M. A.; Sevink, G. J. A. *J. Chem. Phys.* **2000**, *112*, 2452–2462.
- Rankin, S. E.; Malanoski, A. P.; van Swol, F. B. *Mater. Res. Soc. Symp. Proc.* **2001**, *636*, 121–126.
- Huang, E.; Rockford, L.; Russell, T. P.; Hawker, C. J. *Nature* **1998**, *395*, 757–758.
- Huang, E.; Russell, T. P.; Harrison, C.; Chaikin, P. M.; Register, R. A.; Hawker, C. J.; Mays, J. *Macromolecules* **1998**, *31*, 7641–7650.
- Thurn-Albrecht, T.; Steiner, R.; DeRouchey, J.; Stafford, C. M.; Huang, E.; Bal, M.; Tuominen, M.; Hawker, C. J.; Russell, T. P. *Adv. Mater.* **2000**, *12*, 787–791.
- Jeong, U.; Ryu, D. Y.; Kho, D. H.; Kim, J. K.; Goldbach, J. T.; Kim, D. H.; Russel, T. P. *Adv. Mater.* **2004**, *16*, 533–536.
- Yang, H.; Coombs, N.; Sokolov, I.; Ozin, G. A. *J. Mater. Chem.* **1997**, *7*, 1285–1290.
- Pai, R. A.; Humayun, R.; Schulberg, M. T.; Sengupta, A.; Sun, J. N.; Watkins, J. J. *Science* **2004**, *303*, 507–510.
- Cagnol, F.; Grosso, D.; Soler-Illia, G. J. A. A.; Crepaldi, E. L.; Babonneau, F.; Amenitsch, H.; Sanchez, C. J. *Mater. Chem.* **2003**, *13*, 61–66.
- Zhao, D.; Yang, P.; Melosh, N.; Feng, J.; Chmelka, B. F.; Stucky, G. D. *Adv. Mater.* **1998**, *10*, 1380–1385.
- Hillhouse, H. W.; Egmond, J. W.; Tsapatsis, M.; Hanson, J. C.; Larese, J. Z. *Microporous Mesoporous Mater.* **2001**, *44–45*, 639–643.